J Mater Sci: Mater Med (2010) 21:1771–1779
DOI 10.1007/s10856-010-4039-z

In situ synthesis of calcium phosphate-polycaprolactone nanocomposites with high ceramic volume fractions

C. Makarov · I. Gotman · X. Jiang · S. Fuchs · C. J. Kirkpatrick · E. Y. Gutmanas

Received: 13 December 2009 / Accepted: 23 February 2010 / Published online: 9 March 2010
© Springer Science+Business Media, LLC 2010

Abstract Biodegradable calcium phosphate-PCL nanocomposite powders with unusually high ceramic volume fractions (80–95%) and uniform PCL distribution were synthesized by a non-aqueous chemical reaction in the presence of the dissolved polymer. No visible polymer separation occurred during processing. Depending on the reagents combination, either dicalcium phosphate (DCP) or Ca-deficient HA (CDHA) was obtained. CDHA-PCL composite powders were high pressure consolidated at room temperature yielding dense materials with high compressive strengths. Such densification route provides the possibility of incorporating drug and proteins without damaging their biological activity. The CDHA-PCL composites were tested in osteoblastic and endothelial cell line cultures and were found to support the attachment and proliferation of both cell types.

1 Introduction

Bone grafting is a surgical procedure performed by orthopedic surgeons to fill bone voids and to assist in healing injured bones. The existing grafting options, however, suffer from serious limitations. Autografts are limited in supply, and their harvesting is associated with donor site morbidity and prolonged operation time with correspondingly increased costs. Allografts and xenografts also have definite drawbacks such as weak, unpredictable mechanical strength and structure, and a risk of transmission of infection. Because of the above complications, there is an increased demand for synthetic bone graft substitutes. A bone graft substitute is a porous three dimensional structure that acts as a scaffold for the ingrowth of capillaries and new bone tissue. In order to support bone ingrowth, the scaffold should be osteoconductive and have adequate mechanical properties to provide initial stability. Ideally, the scaffold should also be bioresorbable and be replaced, over time, by a new bone. The properties of a porous scaffold are controlled by the scaffold geometry (pore size and interconnectivity) and by the material it is made of. Choice of material will fix the cell-material interaction characteristics as well as the range of mechanical properties that can be achieved. The bulk material will set the maximum mechanical properties that can be achieved [1].

The majority of currently used bone graft substitutes are based on bioactive calcium phosphate (CaP) ceramics, primarily hydroxyapatitie and beta-tricalcium phosphate. The former is considered stable in the body fluids and is resorbed very slowly whereas the latter is resorbed much more quickly. Most importantly, both materials are inherently brittle and cannot be used for healing load-bearing bones. Biodegradable polymers, e.g., polylactic acid (PLA) and polycaprolactone (PCL), are another class of materials considered for resorbable scaffolds. Their use, however, is limited by the low strength and an inflammatory response elicited by the acidic products of their hydrolytic degradation. To produce osteoconductive scaffolds with improved mechanical stability, composites of CaP ceramics and polymers are being developed.

Many polymer-ceramic systems have been studied as materials for bone healing [2–6]. The common feature of practically all the proposed materials is the low volume

C. Makarov · I. Gotman (✉) · E. Y. Gutmanas
Faculty of Materials Engineering, Technion-IIT, Haifa, Israel
e-mail: gotman@tx.technion.ac.il

X. Jiang · S. Fuchs · C. J. Kirkpatrick
Institute of Pathology, Universitätsmedizin der Johannes Gutenberg-Universität, Langenbeckstrasse 1, Mainz, Germany

fraction of the ceramic phase that is utilized in the form of dispersed particles that reinforce the continuous polymer matrix. In such material design, the main contribution of the ceramic particles is the increased stiffness and better biocompatibility. The strength, on the other hand, does not increase significantly and may even decrease [4, 7]. Despite the desirable properties of calcium phosphate ceramics such as high compressive strength and stiffness, there are no literature reports on the toughening of these brittle materials by the addition of small volume fractions of a polymer phase. We hypothesize that such an approach can yield strong and tough composite materials where the hard ceramic skeleton provides structural consistency and hardness, while the soft polymeric phase acts as a binder and provides a certain degree of ductility and fracture resistance. In addition, nanoscale modifications should provide a more homogeneous microstructure and further improve the mechanical properties.

The standard approach to the processing of bulk ceramic-polymer composites involves the mixing of a pre-synthesized CaP powder with a polymer followed by densification. Ceramic nanoparticles, however, tend to agglomerate already during synthesis and it is difficult to achieve their homogeneous distribution while mixing with polymer. To obtain a more uniform phase distribution in CaP-polymer composites, an "in situ" processing approach has been recently advocated [8–11]. In this approach, CaP nanocrystals are not pre-synthesized but are formed "in situ" in the presence of polymer. Thus, extensive ceramic particle agglomeration is avoided and higher degree of interaction and bonding between the organic and inorganic components of the composite is achieved, potentially resulting in better mechanical properties.

In addition to mechanical properties improvement, many research efforts focus on the development of scaffolds with drug-delivery capacity. Local release of osteoinductive growth factors from the scaffold might guide cells to differentiate towards enhanced bone production thus speeding up the regeneration of functional tissue at the site of injury. The incorporation of biomolecules does not allow high temperatures (>50°C) or extremely aggressive chemical conditions during processing. Unfortunately, most currently used industrial or laboratory fabrication routes employ relatively high temperatures to obtain dense calcium phosphate-bioresorbable polymer composites [4, 5]. Consolidation techniques based on higher pressures can produce dense materials at near-room temperatures and are less likely to be harmful for biomolecules.

The present paper reports the fabrication of novel bioresorbable calcium phosphate-PCL (polycaprolactone) nanocomposites with high volume fractions of the ceramic phase by in situ synthesis of the composite powder followed by high pressure consolidation at room temperature—cold sintering [12]. Initial studies on biocompatibility of these novel scaffold materials using osteoblastic and endothelial cell lines are performed to assess their potential as a scaffolding material in bone tissue engineering.

2 Experimental details

2.1 Materials

Dried calcium acetate $(CH_3COO)_2Ca$ (Spectrum Chemical Mfg. Corp., USA), solid O-phosphoric acid, H_3PO_4 (99%, Riedel–deHaen, Seelze, Germany) and Sodium methoxide, $NaOCH_3$ (97%, Fluka, Germany) were used as reactants for calcium phosphate synthesis. Anhydrous tetrahydrofurane (THF) (99.9%, Aldrich) was used as a solvent. Poly(ε-caprolactone) (PCL), 3 mm pellets, mean Mw > 100,000, $\rho = 1.1$ g/cm^3, $T_m = 58$–60°C, was purchased from Solvay Caprolactones, U.K.

2.2 Composite powder synthesis

The starting point for the one-pot synthesis of Ca phosphate-PCL composite powder was a reaction between calcium acetate, $CaAc_2$ and phosphoric acid earlier reported for the synthesis of beta-tricalcium phosphate, β-TCP in methanol [13]:

$$3Ca(OOCCH_3)_2 + 2H_3PO_4 \leftrightarrow Ca_3(PO_4)_2 + 6CH_3COOH \quad (1)$$

Since PCL is practically insoluble in methanol, THF was used as the reaction medium capable of dissolving the PCL polymer. In brief, H_3PO_4 was dissolved in THF after which $CaAc_2$ was added while stirring. Once the difficulty of obtaining β-TCP by the direct reaction between Ca acetate and phosphoric acid had been established, several process modifications were attempted. The procedure that was finally decided upon involved the addition of an organic sodium base, sodium methoxide, $NaOCH_3$ as an intermediate step, the planned reaction sequence being:

$$H_3PO_4 + 3NaOCH_3 \leftrightarrow Na_3PO_4 + 3CH_3COH \quad (2a)$$

$$2Na_3PO_4 + 3Ca(OOCCH_3)_2 \leftrightarrow Ca_3(PO_4)_2 + 6NaCOOH \quad (2b)$$

Reaction (2a) was used to produce a homogeneous suspension of very fine Na_3PO_4 salt particles to be further transformed into β-TCP by reaction with $CaAc_2$ (2b). For this procedure, the desired amount of PCL (0.5 or 0.87 g corresponding, respectively, to 11 and 24 vol.% in the final product) was first mixed with 90 ml THF in a 250 ml reaction bottle with a glass-coated magnetic bar and stirred for 15 min until completely dissolved. Then, 4.909 g

H_3PO_4 were added followed by 8.106 g $NaOCH_3$. After 0.5–1 h vigorous stirring (temperature decreased to ambient), 11.87 g $CaAc_2$ were added slowly (minutes) in the same manner. Finally, 50 ml THF were added and the reaction bottle sealed. The whole procedure was performed in a dry nitrogen flow. After a predetermined time period (up to 4 days), the bottle was unsealed and left open for 24 h to evaporate THF. The reaction product was triple rinsed in double distilled water (DDW) and centrifuged to dissolve the sodium salt by-product and calcium acetate residues and separate them from the calcium phosphate-PCL powder. The obtained powder was dried under vacuum for 2 days and crushed in a mortar to disintegrate agglomerates.

2.3 Powder consolidation

The synthesized composite powders were high pressure consolidated at room temperature (cold sintered [12]) in rigid dies made of a high-speed tool steel at 2.5 GPa in a Toni Technik Press. The punches and inner surfaces of the dies were mirror polished. The specimens were 10.7 mm in diameter (D) and 1 mm high (for cell culture tests) and 4 mm diameter (H) (for compression test). In addition, several specimens with $D = 6.2$ mm and $H = 10$ mm were prepared for compression test.

2.4 Material characterization

Microstructure characterization of synthesized and consolidated nanocomposite powder was performed in a high-resolution scanning electron microscope, HRSEM (Leo Gemini 982) using the accelerating voltage of 4 kV. Phase identification was done by X-ray diffraction, XRD in an automatic powder Philips PW-1820 diffractometer with a long-focus Cu K_α tube operating at 40 kV and 40 mA. Step scans were taken with a 0.25° step and a 10 s exposure.

The density of consolidated materials was measured by dividing the specimen mass by its volume. For estimations of relative density, the theoretical density of Ca-deficient hydroxyapatite was taken as 2.95 g/cm^3.

Compression tests were performed in an Instron testing machine, Model 1195, at the crosshead speed of 0.01 mm/min for the 4 mm high specimens and 0.02 mm/min for the 10 mm high specimens, resulting in the strain rate of about 2×10^{-5} s^{-1}. The anvils of the testing machine were sprayed with a Teflon-like dry lubricant to reduce friction at the contact surfaces.

2.5 Biocompatibility tests

2.5.1 Selected cell lines and corresponding cell culture medium

Two endothelial cell lines, ISO-HAS and HPMEC-ST1.6R and 2 osteoblastic cell lines, MG-63 and Saos-2 were used to test the general biocompatibility of CDHA-PCL disks. The sources of the cell lines are listed in Table 1. ISO-HAS cells were cultured in RPMI-1640 medium (supplemented with GlutaMAX-I, Invitrogen GmbH, Karlsruhe, Germany) containing 10% (v/v) FCS (Sigma–Aldrich Chemie GmbH, Steinheim, Germany) and 100 μg/ml penicillin/streptomycin (Invitrogen GmbH, Karlsruhe, Germany); HPMEC-ST1.6R cells were cultured in M-199 medium (HEPES modified, Sigma–Aldrich Chemie GmbH, Steinheim, Germany) containing 20% (v/v) of FCS, 25 μg/ml Sodium Heparin (Sigma–Aldrich Chemie GmbH, Steinheim, Germany), 25 μg/ml EC growth supplement (Biomol GmbH, Hamburg, Germany), 2 mM GlutaMAX-I (Invitrogen GmbH, Karlsruhe, Germany), and 100 μg/ml penicillin/streptomycin; MG-63 cells and Saos-2 cells were cultured in DMEM/F-12 medium (Invitrogen GmbH, Karlsruhe, Germany) containing 10% (v/v) FCS and 100 μg/ml penicillin/streptomycin.

2.5.2 Pre-neutralization of CDHA-PCL disks and cell seeding

Before seeding cells, CDHA-PCL disks were placed in 24-well cell culture plates and treated with 70% EtOH for 10 min at room temperature (RT). After that the disks were washed with PBS (Invitrogen GmbH, Karlsruhe, Germany) for 3 times and pre-neutralized in pure M199 medium without serum or supplements for 72 h in 37°C incubator. The pre-neutralized CDHA-PCL disks were then coated with fibronectin (10 μg/ml, Roche Diagnostics GmbH, Penzberg, Germany) at 37°C for 1 h. Then the coated CDHA-PCL disks were transferred into uncoated 24-well

Table 1 Cell lines used for testing the biocompatibility of CDHA-PCL nanocomposites

Cell line	Derived from	Reference or Cat Nr.
HPMEC-ST1.6R	Human pulmonary microvascular endothelial cells (HPMEC) cotransfected with pSV3neo and pC1.neo.hTER	[17]
ISO-HAS	Human hemangiosarcoma	[18]
MG-63	Human osteosarcoma	ATCC® Cat. Nr.CRL-1427
Saos-2	Human osteosarcoma	ATCC® Cat. Nr.HTB-85

plates and 100,000 cells in 1 ml corresponding medium were seeded onto each disk. After being cultivated for 24 h, the disks seeded with cells were transferred to new untreated 24-well cell culture plates to get further cultured. All the 4 cell lines were fed with the corresponding medium every 2 days.

2.5.3 *Calcein-AM viable cell staining and confocal microscopy*

ISO-HAS, HPMEC-ST1.6R, MG-63 and Saos-2 were cultured on CDHA-PCL disks for 48 h (24 h after being transferred to new 24 wells) and 8 days (1 week after being transferred to new 24 wells). At the indicated time points the samples were treated with 2 μg/ml Calcein-AM (Invitrogen GmbH, Karlsruhe, Germany) in corresponding medium in a 37°C incubator for 10 min. The stained samples were immediately analysed by confocal microscopy (Leica TCS SP2, Leica Microsystems, Wetzlar, Germany).

3 Results and discussion

3.1 Material synthesis

3.1.1 *Synthesis by direct reaction between phosphoric acid and Ca acetate*

Figure 1a shows the XRD pattern of a powder obtained by the direct calcium acetate salt-phosphoric acid reaction performed in either pure THF or in THF with dissolved PCL. It can be seen that, instead of the expected β-TCP, the calcium phosphate product is dicalcium phosphate, $CaHPO_4$ (DCP). Small peaks of unreacted calcium acetate can be detected, too. Strong bands of acetate (at 1,400–1,600 cm^{-1}) are also present in the FTIR spectrum, Fig. 2a. This means that the synthesis reaction doesn't proceed to the completion and can be described as:

$$3Ca(OOCCH_3)_2 + 2H_3PO_4 \leftrightarrow 2CaHPO_4 + 2CH_3COOH + Ca(OOCCH_3)_2 \quad (3)$$

The unreacted Ca acetate could be easily removed by water rinsing, leaving behind a mixture of DCP and dicalcium phosphate hydrate (DCPD), Figs. 1b and 2b.

No visible polymer agglomeration or deposition on the reaction vessel walls was observed when synthesis was performed in THF with dissolved PCL suggesting that all the PCL was incorporated in the product powder. The presence of predetermined amounts of polymer in the DCP/DCPD-15 PCL composite powders was further confirmed

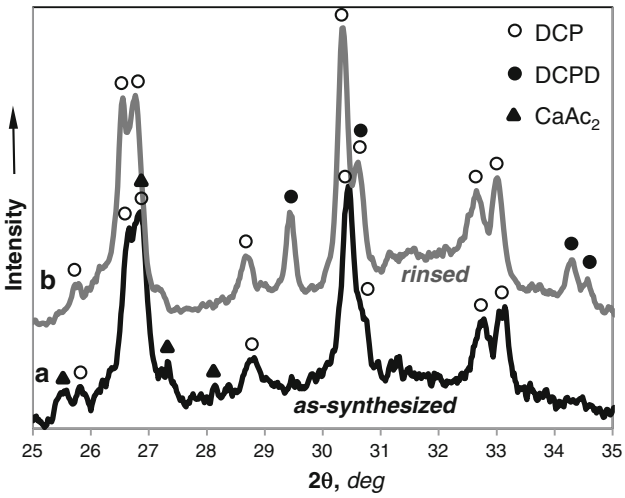

Fig. 1 XRD pattern of the powder synthesized by reaction between phosphoric acid and calcium acetate in THF with dissolved PCL: (*a*) as synthesized; (*b*) water rinsed

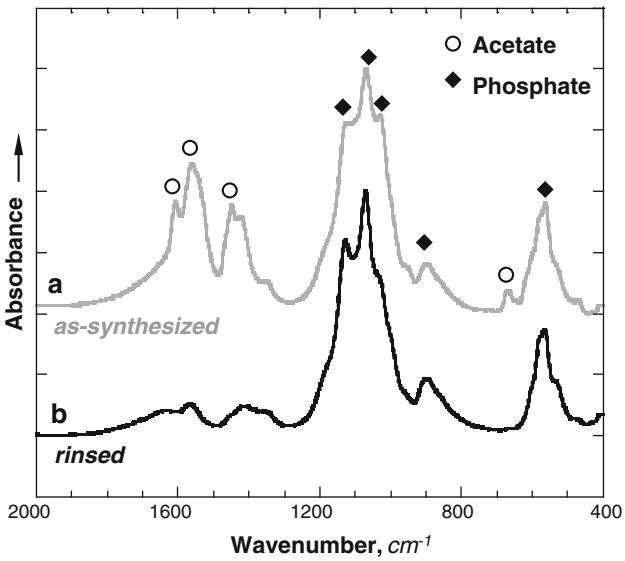

Fig. 2 FTIR spectrum of the powder synthesized by reaction between phosphoric acid and calcium acetate in THF with dissolved PCL: (*a*) as synthesized; (*b*) water rinsed

by the results of double extraction in dichloromethane and ethyl acetate. Figure 3 shows a representative HRSEM image of the DCP/DCPD-15 vol.% PCL composite powder obtained after the removal of residual Ca acetate by water rinsing. Fine submicron (≤500 nm) calcium phosphate particles and, occasionally, thin PCL fibers can be observed. Such DCP/DCPD-PCL composite powders could become a useful material for fabrication of bioresorbable implants. The dissolution rate of such implants, however, could be too high for bone healing applications due to the rapid dissolution of the DCP/DCPD component. Therefore, the synthesis route of CaP-PCL composites by direct

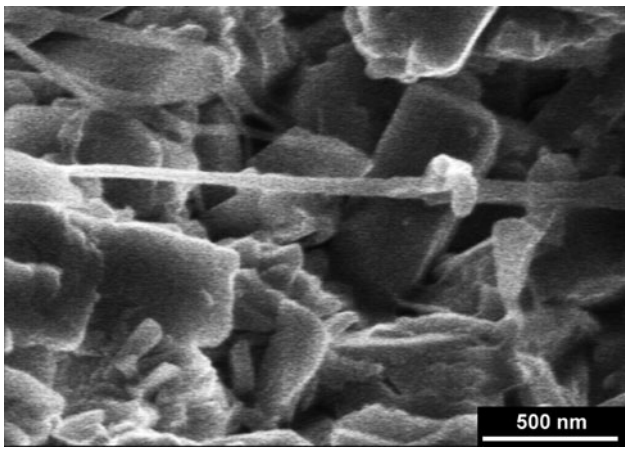

Fig. 3 Representative HR-SEM image of the composite DCP/DCPD-15 vol.% PCL composite powder synthesized by reaction between phosphoric acid and calcium acetate

reaction between Ca acetate and phosphoric acid was not further pursued.

3.1.2 *Synthesis by reaction between phosphoric acid, sodium methoxide and Ca acetate*

According to XRD analysis, the reaction between sodium methoxide, phosphoric acid and calcium acetate (Eqs. 2a, 2b) in THF, with or without dissolved PCL, produced, after 1–24 h stirring, an increasing amount of sodium acetate hydrate ($NaAc{\cdot}3H_2O$) and decreasing amounts of sodium phosphate and calcium acetate hydrate ($CaAc_2{\cdot}0.5H_2O$). No evidence of polymer phase separation was observed during processing. After 2 days of stirring, calcium acetate reagent was no longer detected in the XRD pattern, Fig. 4a. On the other hand, the peaks of the sodium acetate product were so strong that they concealed almost completely the shallow peaks of Ca phosphate. Removing the water-soluble components left behind a very fine white powder being, according to XRD, a pure calcium phosphate (Fig. 4b). The peak positions in the XRD pattern in Fig. 4b, however, don't correspond to the expected β-TCP but fit rather closely those of hydroxyapatite (HA), $Ca_{10-x}(HPO_4)_x(PO_4)_{6-x}(OH)_{2-x}$. The peaks are broad and shallow suggesting a very fine nanocrystalline structure of the synthesized HA.

The stoichiometry of hydroxyapatite (the value of x) is important as it strongly affects the material's solubility. Stoichiometric HA, $Ca_{10}(PO_4)_6(OH)_2$ ($x = 0$) is practically insoluble in the body fluids, whereas the solubility of Ca-deficient HA (CDHA) increases with increasing x approaching that of β-TCP at $x = 1$ [14]. Although XRD patterns of HA and CDHA are very similar, the two compounds can be easily distinguished if heated above 700°C: the stoichiometric HA will remain unchanged

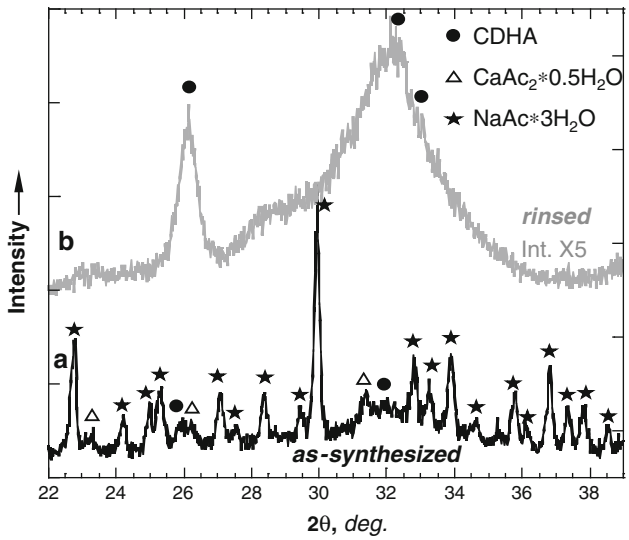

Fig. 4 XRD pattern of as-synthesized (*a*) and water rinsed (*b*) CaP-11PCL powder obtained by reaction between phosphoric acid, sodium methoxide and Ca acetate. Similar patterns were obtained for CaP-24PCL and pure CaP powders synthesized in the same way

whereas CDHA will transform into a mixture of HA and β-TCP for ($0 < x < 1$) or pure β-TCP (for $x = 1$). Our synthesized powder, when annealed at 700°C, 30 min, transformed almost completely in β-TCP, Fig. 5, implying that the materials is a Ca-deficient HA with x slightly less than unity. It is believed that the formation of CDHA instead of the planned β-TCP occurs due to some water absorption by the strongly hygroscopic sodium methoxide and can be described by the following reaction:

$$H_3PO_4 + NaOCH_3 + Ca(OOCCH_3)_2 + H_2O \leftrightarrow Ca_{10-x}(HPO_4)_x(PO_4)_{6-x}(OH)_{2-x} + NaCOOH + CH_3COH \quad (3)$$

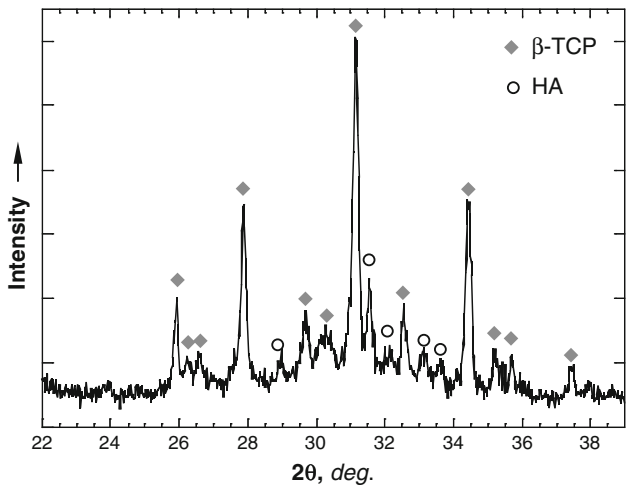

Fig. 5 XRD pattern of water rinsed CaP-11PCL powder after annealing at 700°C, 30 min

Table 2 Properties of the synthesized CDHA-PCL nanocomposites

Designation	Nominal PCL fraction (vol.%)	Measured PCL fraction (vol.%)	Relative density (%)	Compressive strength, σ_c (MPa)
CDHA-11PCL	11	5	~88	128 ± 4
CDHA-24PCL	24	14	~91	142 ± 5

The yield of synthesized CDHA powder increased with stirring time leveling off after approximately 2 days. Assuming $x = 1$, the amount of CDHA obtained in pure THF (without dissolved PCL) corresponded to near 100% conversion of the reagents according to Eq. 3.

The amount of PCL in the CHDA/PCL composite powders (extracted by double extraction in dichloromethane and ethyl acetate) was found to be lower than the amount initially dissolved in THF, see Table 2. It is assumed that the addition of a strongly basic sodium methoxide to THF causes chain scission of dissolved PCL and the resulting low molecular weight fragments are removed during subsequent water rinsing.

In Fig. 6, high resolution SEM images of the synthesized CDHA-PCL powder are presented. The powder has a very fine nanoscale needle-like morphology typical of CDHA [15]. The polymer phase is difficult to detect suggesting its homogeneous distribution. Occasionally, thin polymer fibers, Fig. 6b (arrows) or thin polymer strips decorated with CaP nanocrystals, Fig. 6d (arrows) can be observed.

Room temperature consolidation of CDHA-11PCL and CDHA-24PCL powders at 2.5 GPa yielded relatively dense composite materials with porosity not exceeding 12%, Table 2. No visible pores were detected in HRSEM, Fig. 7, suggesting that either the pores are extremely fine (nanometers) or that polymer flow during high-pressure consolidation results in pore closure on the tablet surface. The compression strength, σ_c, of the CDHA-11PCL and CDHA-24PCL specimens was about 130 and 145 MPa, respectively, Table 2. A similar compression behavior was recorded for the 4 mm high (H/D $\approx$ 0.4) and 10 mm high (H/D $\approx$ 1.6) specimens apparently due to homogenous compression (no friction present at the contact surfaces).

3.2 Biocompatibility of CDHA-PCL nanocomposites

In order to gain insight if CDHA-PCL disks support the growth of the two highly relevant cell types in bone tissue engineering two endothelial cell lines, ISO-HAS and HPMEC-ST1.6R and two osteoblastic cell lines, MG-63 and Saos-2 were cultured on CDHA-PCL disks for 48 h or 8 days followed by calcein-Am viability staining and confocal microscopy. In Fig. 8, on both variants of materials ISO-HAS and HPMEC-ST1.6R cells grew to

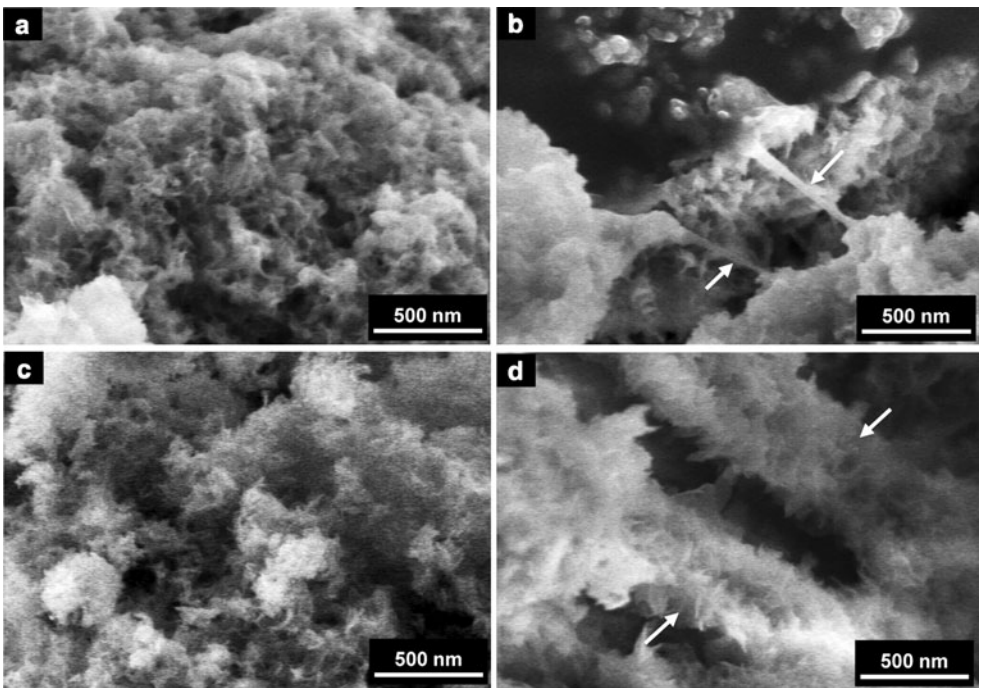

Fig. 6 Representative HR-SEM micrographs of the synthesized CDHA-11PCL (**a**, **b**) and CDHA-24PCL (**c**, **d**) composite powders

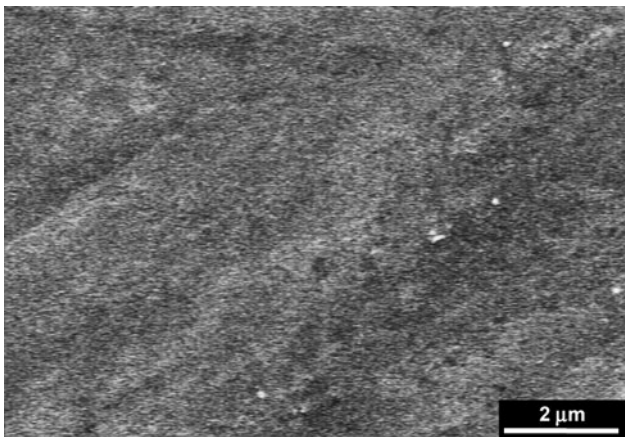

Fig. 7 HR-SEM micrograph of high pressure consolidated CDHA-11PCL composite

sub-confluence after 48 h of culture (A, C, E, G) and reached confluence after 8 days (B, D, F, H). In case of osteogenic cell lines (Fig. 9), MG-63 and Saos-2 cells grew to confluent cell layers on both CDHA-11PCL and CDHA-24PCL disks during the first 48 h (A, C, E, G). This confluent state was maintained after 8 days of culture (B, D, F, H).

ISO-HAS attached on both variants of materials after 48 h, though more adhered cells were observed on CDHA-11PCL disks compared to the CDHA-24PCL. Further, during 8 days of culture ISO-HAS proliferated resulting in similar levels of confluency on both types of materials. This result indicates that both CDHA-11PCL and CDHA-24PCL nanocomposites support the attachment and proliferation of ISO-HAS, although CDHA-11PCL appeared to be beneficial for ISO-HAS adherence in this early stage of the culture. Similarly, another endothelial cell line HPMEC-ST1.6R grew to sub-confluence after 48 h and into confluent cell layers after 8 days, indicating no significant difference between the two material variants. The experiments described above were performed with FN-coated materials. Endothelial cells attach to some extent also on uncoated nanocomposites (data not shown), nevertheless uncoated disks lead to a higher experimental variation in cell attachment which is particulary critical in terms of primary endothelial cells and further studies on the effect of PCL content on cell behavior [16].

Concerning the osteoblastic cell lines, MG-63 and Saos-2 cells grow into confluent layers within 48 h. After 8 days, both MG-63 and Saos-2 cells formed super-confluent cell layers on both CDHA-11PCL and CDHA-24PCL disks. Additionally, we observed no difference between the two material variants in confocal microscopy in terms of cell attachment or cell proliferation.

Further studies assessed the biocompatibility of these nanocomposites using primary osteogenic cells including also the assessment of osteogenic differentiation. In this context both material variants were investigated using monocultures of primary endothelial cells and primary human osteoblasts, as well as co-cultures of osteoblast and

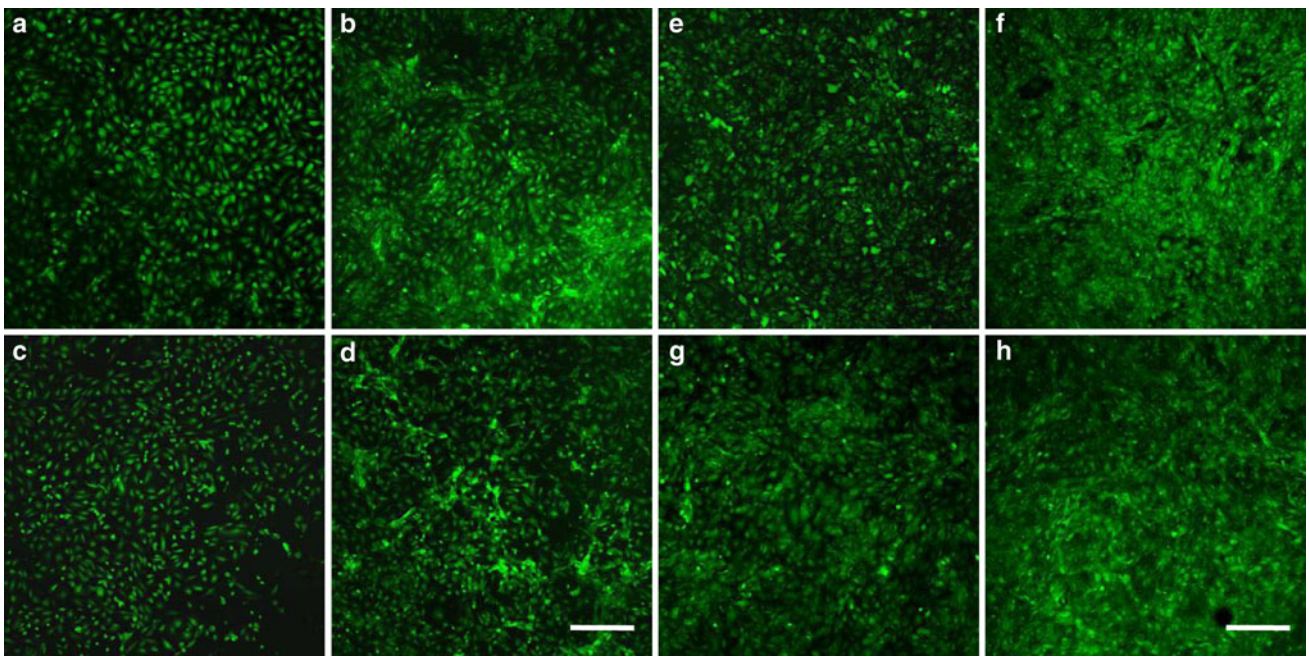

Fig. 8 Biocompatibility of CDHA-PCL disks to endothelial cell lines. ISO-HAS (**a**–**d**) and HPMEC-ST1.6R (**e**–**h**) cells were cultured on CDHA-11PCL disks (**a**, **b**, **e**, **f**) and CDHA-24PCL disks (**c**, **d**, **g**, **h**) for 48 h (**a**, **c**, **e**, **g**) and 8 days (**b**, **d**, **f**, **h**) and assessed by confocal microscopy staining with Calcein-AM (*green*). Scale bar = 300 µm. (Color figure online)

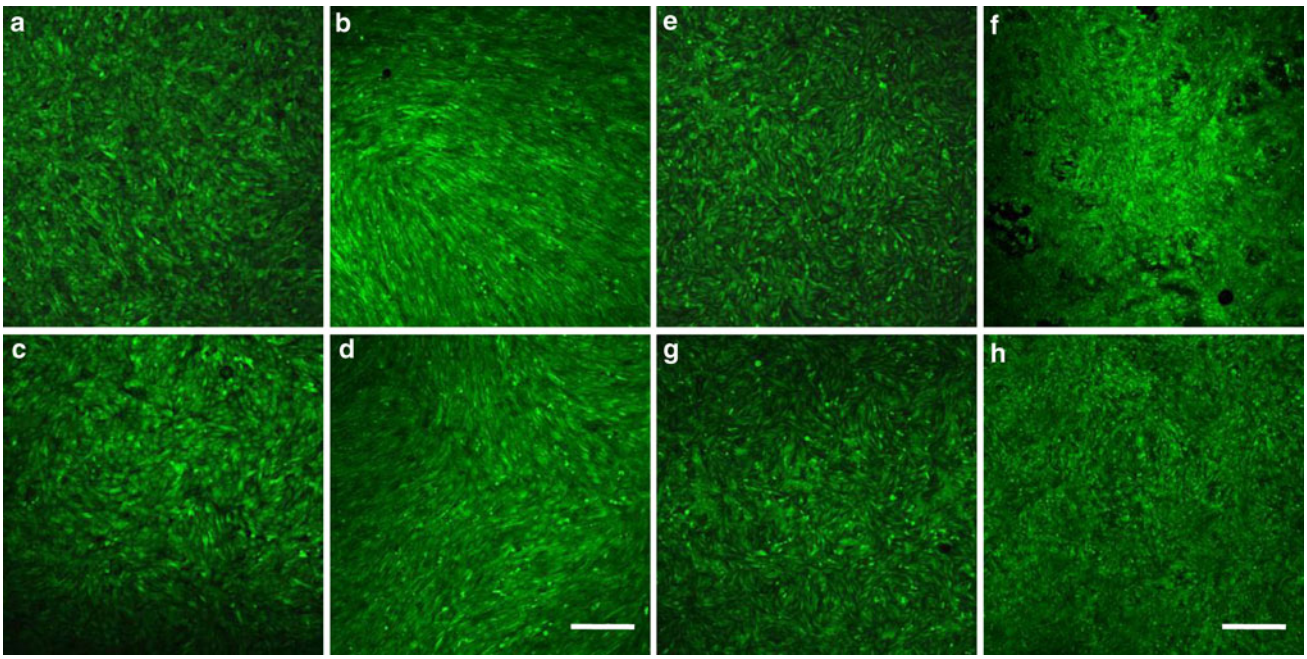

Fig. 9 Biocompatibility of CDHA-PCL disks to osteoblastic cell lines. MG-63 (**a**–**d**) and Saos-2 (**e**–**h**) cells were cultured on CDHA-11PCL disks (**a**, **b**, **e**, **f**) and CDHA-24PCL disks (**c**, **d**, **g**, **h**) for 48 h (**a**, **c**, **e**, **g**) and 8 days (**b**, **d**, **f**, **h**) and assessed by confocal microscopy staining with Calcein-AM (*green*). Scale bar = 300 μm. (Color figure online)

endothelial cells to assess a potential influence of the polymer-content on tissue engineered constructs of the bone. In summary the here presented data using cell lines and the data gained from primary cells suggest the biocompatibility of the CDHA-PCL nanocomposites for osteoblastic and endothelial cells.

4 Conclusions

Calcium phosphate-PCL nanocomposite powders with high ceramic volume fractions (80–95%) were successfully synthesized by a non-aqueous chemical reaction in the presence of the dissolved polymer. Depending on the reagents combination used (calcium acetate, phosphoric acid and sodium methoxide), different Ca phosphates (dicalcium phosphate (DCP)-PCL or Ca-deficient HA (CDHA), both considered bioresorbable) were obtained. The process leading to the formation of DCP allowed full incorporation of the dissolved polymer in the composite whereas roughly 50% of the total polymer amount was incorporated in the CDHA-PCL material. Despite the very low PCL fractions, a uniform distribution of the polymer phase has been achieved.

The CDHA-PCL composite powders obtained were high-pressure consolidated into dense materials at room temperature at 2.5 GPa. The advantage of the process is the possibility of incorporating biomolecules (drugs, growth factors) already during fabrication. CDHA-based composites nominally containing 11 and 24 vol.% PCL exhibited high strengths and supported the attachment and proliferation of endothelial and osteoblastic cell lines. These properties make the synthesized nanocomposites attractive materials for bioresorbable scaffold fabrication. Degradation studies of the CDHA-PCL composites are currently underway. Future studies will focus on fabrication of porous scaffolds from the synthesized CDHA-PCL composite powders.

Acknowledgments The research was supported by U.S.-Israel Binational Science Foundation (BSF) through research grant No. 2004-293.

References

1. Hollister SJ, Liao EE, Moffitt EN, Jeong CG, Kemppainen JM. Defining design targets for tissue engineering scaffolds. In: Meyer U, Meyer T, Handschel J, Wiesmann HP, editors. Fundamentals of tissue engineering and regenerative medicine. Berlin: Springer; 2009. p. 521–37.
2. Rezwan K, Chen QZ, Blaker JJ, Boccaccini AR. Biodegradable and bioactive porous polymer/inorganic composite scaffolds for bone tissue engineering. Biomaterials. 2006;27:3413–31.
3. Dorozhkin SV. Calcium orthophosphate-based biocomposites and hybrid biomaterials. J Mater Sci. 2009;44:2343–87.
4. Shikinami Y, Okuno M. Bioresorbable devices made of forged composites of hydroxyapatite (HA) particles and poly-L-lactide (PLLA): Part I Basic characteristics. Biomaterials. 1999;20:859–77.
5. Ignjatovic N, Suljovrujic E, Budinski-Simendic J, Krakovsky I, Uskokovic D. Evaluation of hot-pressed hydroxyapatite/poly-L-

lactide composite biomaterial characteristics. J Biomed Mater Res. 2004;71B:284–94.
6. Neumann M, Epple M. Composites of calcium phosphate and polymers as bone substitution materials. Eur J Trauma. 2006;2: 125–31.
7. Bleach NC, Nazhat SN, Tanner KE, Kellomäki M, Törmälä T. Effect of filler content on mechanical and dynamic mechanical properties of particulate biphasic calcium phosphate-polylactide composites. Biomaterials. 2002;23:1579–85.
8. Hakimimehr D, Liu DM, Troczynski T. In situ preparation of poly(propylene fumarate)-hydroxyapatite composite. Biomaterials. 2005;26:7297–303.
9. Ambrosio AMA, Sahota JS, Khan Y, Laurencin CT. A novel amorphous calcium phosphate polymer ceramic for bone repair: I. Synthesis and characterization. J Biomed Mater Res. 2001;B58: 295–301.
10. Choi D, Marra KG, Kumta PN. Chemical synthesis of hydroxyapatite/poly(ε-caprolactone) composites. Mater Res Bull. 2004; 39:417–32.
11. Petricca SE, Marra KG, Kumta PN. Chemical synthesis of poly(lactic-co-glycolic acid)/hydroxyapatite composites for orthopaedic applications. Acta Biomater. 2006;2:277–86.
12. Gutmanas EY. Cold sintering—high pressure consolidation. In: ASM handbook, vol. 7, "powder metal technologies and applications". Materials Park: ASM International; 1998. pp. 574–82.
13. Bow JS, Liou SC, Chen SY. Structural characterization of room-temperature synthesized nano-sized β-tricalcium phosphate. Biomaterials. 2004;25:3155–61.
14. Bohner M. Calcium orthophosphates in medicine: from ceramics to calcium phosphate cements. Injury. 2000;31:S-D37–D47.
15. Liou SC, Chen SY, Liu DM. Phase development and structural characterization of calcium phosphate ceramics-polyacrylic acid nanocomposites at room temperature in water-methanol mixtures. J Mater Sci. 2004;15:1261–6.
16. Fuchs S, Jiang X, Gotman I, Makarov C, Schmidt H, Gutmanas EY, Kirkpatrick CJ. Influence of polymer content in Ca-deficient hydroxyapatite-polycaprolactone (CDHA-PCL) nanocomposites on the formation of microvessel-like structures. Acta Biomater. 2010; on-line.
17. Krump-Konvalinkova V, Bittinger F, Unger RE, Peters K, Lehr HA, Kirkpatrick CJ. Generation of human pulmonary microvascular endothelial cell lines. Lab Investig. 2001;81:1717–27.
18. Masuzawa M, Fujimura T, Hamada Y, Fujita Y, Hara H, Nishiyama S, et al. Establishment of a human hemangiosarcoma cell line (ISO-HAS). Int J Cancer. 1999;81:305–8.